Carbohydrate Polymer Technologies and Applications 11 (2025) 100918

Contents lists available at ScienceDirect

Carbohydrate Polymer Technologies and Applications

journal homepage: www.sciencedirect.com/journal/carbohydrate-polymer-technologies-and-applications

Effects of chitosan thin barrier layers on the oxygen permeability and optical properties of poly(lactic acid) and poly (3-hydroxybutyrate-co-3-hydroxyvalerate) multilayers

I. Bernabé Vírseda [a,*], M.U. de la Orden [b], J. Martínez Urreaga [a]

[a] Departamento de Ingeniería Química Industrial y del Medio Ambiente, E.T.S.I.I., Universidad Politécnica de Madrid, José Gutiérrez Abascal 2, 28006 Madrid, Spain
[b] Departamento de Química Orgánica, Universidad Complutense de Madrid, Facultad de Óptica y Optometría, Arcos de Jalón 118, 28037 Madrid, Spain

ARTICLE INFO

Keywords:
Chitosan
PLA
PHBV
Surface activation
O_2 permeability
Optical properties

ABSTRACT

Poly(3-hydroxybutyrate-co-3-hydroxyvalerate) (PHBV) and poly(lactic acid) (PLA) are highly promising bio-based and biodegradable polymers in food packaging industry due to their mechanical and optical properties, and improved sustainability. Nevertheless, some properties like O_2 permeability need improvement. In this work we have prepared and tested bilayers from PLA and blends of PLA and PHBV, with an additional thin layer of chitosan (CH) to reduce the oxygen transmission rate (OTR) without compromising optical properties. In these materials, the poor compatibility between hydrophilic CH and hydrophobic biopolymers is a serious handicap, as it leads to weak adhesion between the layers. The hydrophobic polymer surfaces were activated with aqueous NaOH at room temperature for different times, which increased hydrophilic character. Considering that bio-polyesters can undergo NaOH-catalised hydrolytic degradation, the effect of NaOH treatment on the structure of the polymers was also studied by using FT-IR spectroscopy, scanning electron microscopy (FE-SEM), micro-hardness and contact angle measurements. Both the use of PHBV and a thin layer of CH lead to significant decreases in O_2 permeability. The decrease is greater in the case of the inner CH layer, which also reduces UV transmittance without significantly affecting the transparency of the film.

1. Introduction

Food packaging plays a vital role in current society since it is of the utmost importance in the food supply chain. Nowadays, plastics are essential in food packaging industry due to different advantages such as, among others, low price and density, ease of processing, good mechanical and optical properties, biocompatibility and printability (Kan & Miller, 2022; Sundqvist-Andberg & Åkerman, 2021). The use of multilayer films leads to high performance in terms of barrier properties for oxygen, water vapor, fats, etc. (Anukiruthika et al., 2020; Laufer et al., 2013). Thus, plastic containers are suitable for marketing and highly effective in preserving the properties of food and increasing its shelf life. The use of plastics in food packaging also has two well-known disadvantages. On the one hand, there is a clear lack of sustainability since most of the plastics used come from non-renewable sources and only a small fraction of these plastics is recycled. According to Plastic Europe, conventional polymers production includes 90.4 % of all the plastic produced worldwide in 2023, which is 413.8 Mt (Plastics Europe, 2024). On the other hand, plastic packaging waste in the environment contributes to important environmental problems such as the generation of micro and nanoplastics and the release of additive residues, some of them potentially toxic, into the environment (Ncube et al., 2020). In addition, the use of some plastics is related to problems of migration of additives and microplastics to the food contained in the packaging (Kumar et al., 2024; Najahi et al., 2025; Yin et al., 2025).

Within this context, part of the solution is using biobased and biodegradable polymers instead of conventional polymers in food packaging. Among the advantages, the use of biobased polymers reduces the carbon footprint because they are derived from renewable resources. Biodegradable polymers have, in general, lower environmental impact than conventional ones because they are more easily degraded and assimilated by environmental microorganisms (Bernabé Vírseda et al., 2024; Maga et al., 2019; RameshKumar et al., 2020). However, the main gap for the replacement of conventional polymers founds on the poor properties of many biobased and biodegradable polymers. Therefore, it is necessary to design biopolymeric structures that equal or exceed the

* Corresponding author.
E-mail address: i.bernabe@upm.es (I. Bernabé Vírseda).

https://doi.org/10.1016/j.carpta.2025.100918

Available online 25 June 2025

properties of conventional polymers, both in terms of barrier properties and in optical, antimicrobial, thermal and mechanical properties (Bernabé et al., 2024; Hamad et al., 2015).

Among all biobased and biodegradable polymers, poly(lactic acid) (PLA) offer notorious advantages in food packaging industry because of its moderate price, biocompatibility and good optical properties (Beltrán et al., 2020; Stefaniak & Masek, 2025). Despite the worldwide production of bioplastics in 2023 is only the 0.7 % of the global plastic production (Plastics Europe, 2024), the production of PLA is increasing, from around 200 kt in 2016 to 459 kt in 2022, and an expected growth of 12 % annually from 2021 to 2026 (Teixeira et al., 2023). Nevertheless, PLA show some drawbacks in its use in food packaging related to its brittleness and low oxygen barrier, in comparison with conventional polymers (Hosseini et al., 2022; Stefaniak & Masek, 2025).

Many strategies have been studied to improve PLA properties relevant for food packaging (Marano et al., 2022; Râpă et al., 2016). Ghasemi et al. reported that the addition of 3 % of talc as nucleating agent for PLA resulted in a decrease around 30 % in the gas permeability of oxygen, carbon dioxide and nitrogen (Ghassemi et al., 2017). A different strategy is the blending of PLA with biofillers or other biodegradable polymers such as starch, lignin, polycaprolactone (PCL), poly(butylene succinate) (PBS) and polyhydroxyalkanoates (PHAs). Zembouai et al. proved that if PLA is blended with 25 wt. % of PHBV, the water and oxygen permeability coefficients decrease around 35 % and 23 %, respectively (Zembouai et al., 2013). Another common strategy is based on the use of polymeric coatings (Claro et al., 2016). Stoleru et al. observed a drop down about 55 % of oxygen permeability of PLA after coating with chitosan (CH) (Stoleru et al., 2021).

In this work we have evaluated the use of coatings and thin layers of chitosan to reduce permeability. Chitosan (CH) is a linear polysaccharide composed mainly of randomly distributed β-(1→4)-linked d-glucosamine (deacetylated unit) and N-acetyl-d-glucosamine (acetylated unit) (See Fig. 1) (Priyadarshi & Rhim, 2020). It is obtained from the deacetylation of chitin in alkaline conditions (Li et al., 2020; H. Wang et al., 2018). Due to the chemical structure, chitosan derived materials are useful for tissue engineering, drug delivery, water treatment, and other applications (Pawariya et al., 2023, 2024; Rabeie et al., 2024). The incorporation of a chitosan layer onto polymeric materials promotes the antimicrobial properties against fungi, moulds, yeasts and bacteria, and also provides excellent barrier properties against oxygen due to its high crystallinity and the hydrogen bonds that form between its molecular chains (Haghighi et al., 2020; Park et al., 2012).

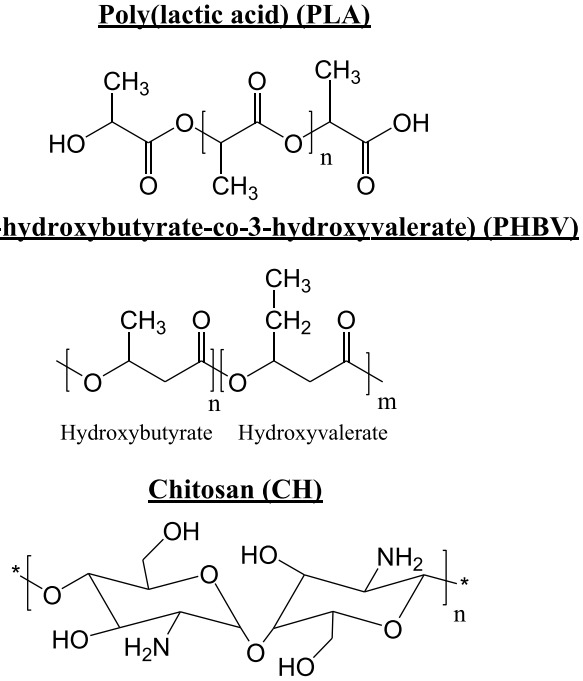

Fig. 1. Chemical structures of the polymers chosen for this research.

The use of chitosan to reduce the permeability is promising but the main issue is the poor compatibility with the hydrophobic PLA, so, it requires the modification of the PLA surface to make it more hydrophilic and, compatible with chitosan. Different solutions are reported in the literature to improve the compatibility between chitosan and PLA.(Li et al., 2020; Vesel, 2023; Yovcheva et al., 2018). In general, surface modification of PLA with coatings, plasma treatment, radiation and photo-grafting are effective but requires expensive instrumentation, which is a notorious disadvantage (Schneider et al., 2020). There are other more affordable techniques, such as treatment with sodium hydroxide (NaOH), which is a cheap and easy-to-perform alternative that causes hydrolysis of the PLA surface(Scaffaro et al., 2019). Mohd Sabee et al. treated PLA with an NaOH aqueous solution and found an effective surface modification which promotes the formation of hydrophilic functional groups and biocompatibility (Mohd Sabee et al., 2016). Andrade-del Olmo et al. reported that immersion of PLA during 30 min in 0.25 M NaOH aqueous solution at 58 °C, improved adhesion to CH (Andrade-Del Olmo et al., 2019). Despite these encouraging results, the treatment of PLA (and its mixtures with other biopolyesters) with NaOH is still poorly understood. It is necessary to study the degradation of the polymer during the treatment, which could have harmful effects on the properties of the material, in order to optimise the processing conditions. In this work, the biopolymer sheets were previously treated with NaOH for improving the adhesion of chitosan. Short treatment times at 25 °C were selected to minimise polymer degradation. The effects of treatment with NaOH on the surface and the degradation of the polymers were studied by FTIR spectroscopy, thermal analysis, FE-SEM and measurements of microhardness and contact angle.

The second alternative used in this work to reduce the oxygen permeability of PLA is based on the use of PHBV, a thermoplastic biopolyester more crystalline than PLA and with lower oxygen permeability (Bernabé et al., 2024; Bernabé Vírseda et al., 2024). The sheet with 25 wt. % of PHBV was selected because it showed the best compatibility to a PLA sheet. The bilayer structures evaluated in this work were prepared from these sheets (Andrade-Del Olmo et al., 2019; Claro et al., 2016; Haghighi et al., 2020; Li et al., 2020; Park et al., 2012; Priyadarshi & Rhim, 2020; Vesel, 2023; H. Wang et al., 2018; Yovcheva et al., 2018).

In this work, different bi and trilayer films were prepared from PLA, chitosan and PLA-PHBV blends, and the effects of PHBV and CH on oxygen permeability and optical properties were measured and analysed. The results of this work provide novel and scientifically relevant information on issues such as the effect of NaOH activation on polymer properties, the combined effect of chitosan coatings and PHBV on PLA permeability, and the effect of these factors on optical properties. These results may contribute to the development of better bio-based materials for more sustainable food packaging.

2. Experimental

2.1. Materials

Commercial plastics PLA (LUMINY® L175), with melt flow index 3 g/10 min (190 °C, 2.16 kg), and PHBV (Y1000), with melt flow index 1–5 g/10 min (190 °C, 2.16 kg), were provided by Nature Plast (France). PLA and PHBV showed an average molecular weight (M_W) of 128.8 ± 0.6 and 156.5 ± 5.5 kDa, respectively, measured by gel permeation chromatography (GPC) using an Agilent 1100 device, using poly(methyl methacrylate) (PMMA) as calibration standards. The eluent was hexafluoro-2-propanol (HFiP) containing 50 mM of potassium trifluoroacetate (CF_3COOK), with a flow rate of 1 mL/min at 30 °C. Lactic acid oligomer (OLA) (Glyplast OLA 2), with viscosity 90 mPa.s (25 °C), was supplied by Condensia (Spain). PLA with 1 wt % of OLA and the

blend composed of PLA (73.5 wt %) and PHBV (24.5 wt %) and OLA (2 wt %), where compounded by Nature Plast (France). Lactic acid (LA) and oligomers of lactic acid (OLA) were used in the dissolution of CH, in an attempt to improve the compatibility of CH with PLA. OLA is a liquid plasticizer for PLA and PHBV that facilitates melt processing and improves the toughness and flexibility of the final material. Only low proportions of OLA were used because bigger proportion of OLA compromise the proper production of the films. The amount of PLA in the blend with PHBV is necessary to ensure good adhesion with PLA films. Plastic films from these materials were produced by extrusion and calendaring at Aimplas (Spain).

Chitosan was supplied by Acros Organics (United States), derived from chitin from crustacea with a degree of deacetylation of 85 %, a specified molecular weight of 100–300 KDa, water content $\leq$ 10 wt % and 0.3 wt % of ash.

2.2. Sample preparation

Multilayer materials were obtained as shown in Fig. 2. The main steps were: a) modification of the polymer surface with NaOH to increase the compatibility with CH; b) preparation of the CH solution with LA and OLA; c) deposition of CH on PLA films by casting; d) incorporation by press moulding of the other polymeric layer (PLA or PLA/PHBV blend). Drying of all samples is carried out in a Thermo Scientific Heraeus Vacutherm oven, coupled with a BUCHI Vacuum Pump V-700.

2.2.1. Surface modification

Pre-activation of the PLA surfaces, which is essential to achieve good adhesion with chitosan, was carried out following a published method (Andrade-Del Olmo et al., 2019), with some modifications. Firstly, the sheets of PLA were washed in a 50 %wt water–methanol mixture, with magnetic stirring for 30 min at room temperature. After drying for 1 hour at 40 °C in a vacuum oven, the activation was performed by submerging the polymer sheets in a 0.25 M NaOH aqueous solution, for 5, 15 or 60 min, with magnetic stirring at 40 °C. Finally, the activated samples were dried for 1 hour at 40 °C in a vacuum oven.

2.2.2. CH application

CH thin films were applied on PLA sheets by solvent casting. CH was dissolved in 2 wt % aqueous solution of LA, using magnetic stirring at room temperature. CH layer thickness was controlled by using different concentrations (1 and 2 wt %) and volume (5.6 and 11.2 mL) of CH. 0.2 wt % OLA was used in some of the formulations to improve compatibility with PLA. After filtering the solution was deposited on the polymer sheet, and then cured. The solvent was removed for 24 h at 40 °C and the final drying was carried out in a vacuum oven during 24 h at 40 °C.

2.2.3. Moulding of polymeric films

The compression moulding was performed in an IQAP LAP (Spain) hot plates press at 150 °C and 100 kg/m^2 of pressure, using 200 μm spacers. Table 1 shows the codenames of the materials studied.

2.3. Characterisation and properties

Characterisation of monolayers and multilayers, as well as the study of the activation processes, were carried by using Fourier Transform Infrared Spectroscopy (FTIR), Differential Scanning Calorimetry (DSC), microhardness and Contact Angle measurements. The crystallinity of

Table 1
Codenames and descriptions of the materials.

Sample	Description
PLA	99 wt % PLA + 1 wt % OLA
Blend	73.5 wt % PLA + 24.5 wt % PHBV + 2 wt % OLA
BlendNa	Blend after activation with NaOH for 5 min
PLANa	PLA after activation with NaOH for 5 min
PLANa-15	PLA after activation with NaOH for 15 min
PLANa-60	PLA after activation with NaOH for 60 min
PLANa-PLANa	Activated PLA + Activated PLA
PLANa-BlendNa	Activated PLA + Activated blend
PLANaCH	Activated PLA + CH deposited on its surface (1 wt % CH and 5.6 mL solution)
PLANa-CHx1v1-PLANa	Activated PLA + CH interlayer (1 wt % and 5.6 mL solution) + Activated PLA
PLANa-COx1v1-PLANa	Activated PLA + CH interlayer (1 wt % CH and 0.2 wt % of OLA and 5.6 mL solution) + Activated PLA
PLANa-CHx1v2-PLANa	Activated PLA + CH interlayer (1 wt % CH and 11.2 mL solution) + Activated PLA
PLANa-CHx2v1-PLANa	Activated PLA + CH interlayer (2 wt % and 5.6 mL solution) + Activated PLA
PLANa-CHx1v1-BlendNa	Activated PLA + CH interlayer (1 wt %- and 5.6-mL solution) + Activated Blend

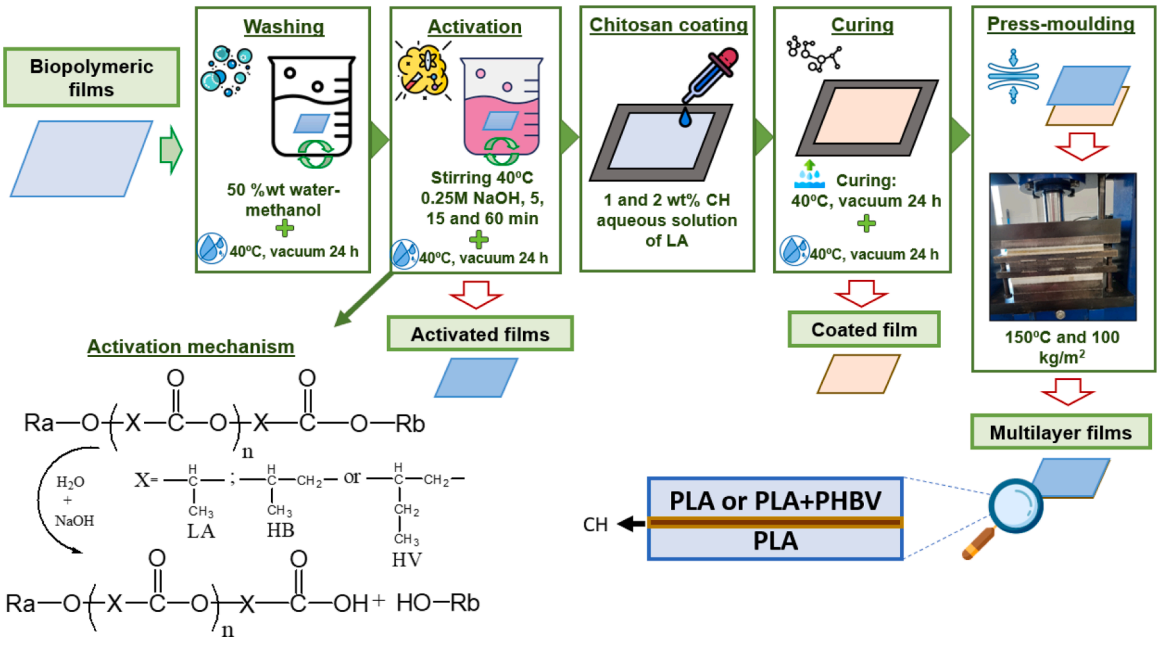

Fig. 2. Scheme of the procedure to obtain multilayer biomaterial.

each sample is estimated from phase transition parameters obtained from DSC, following the equation

$$X = \frac{\Delta H_C}{\Delta H_0} \cdot 100 \quad (1)$$

where X is the crystallinity degree (%) and ΔH_C is the area under the crystallisation exotherm during cooling scan, which correspond to the crystallisation enthalpy. ΔH_0 (J/g) is the melting enthalpy of 100 % crystalline PLA, which has been considered to be 93.1 J/g (Beltrán et al., 2018).

Regarding the FTIR, a Nicolet iS10 spectrometer, equipped with a diamond Attenuated Total Reflectance (ATR) accessory, was used for the characterisation of the single layers. 16 scans at 4.0 cm^{-1} of resolution were averaged. FTIR-ATR spectra were normalised using the 1451 cm^{-1} band as an internal standard reference for PLA reference (Kister et al., 1998). The characterisation of the trilayers by FTIR microspectroscopy and microscopy was performed on a Jasco 4700 spectrometer coupled with an IRT-7100 Microscope, equipped with an MCT detector and an observation lens (X16 Cassagrain). The spectra in ATR mode were recorded using an ATR-5000-SS Clear-View ATR objective with a ZnS prism. 64 scans at 4.0 cm^{-1} of resolution were averaged.

Contact angles (Θ) were measured in a Theta Lite Attention Tensiometer (Biolin Scientific, Gothenburg, Sweden), using the software One Attention. 4 μL deionised water droplets were deposited on dry and plane samples at room temperature. Each contact angle reported is the average of at least 5 measurements. Images were recorded every 10 s.

Scanning electron microscopy (SEM) was performed using a Hitachi FE-SEM SU-8000 to test the morphology of the surfaces and interfaces. The samples were previously coated with a layer of chromium and placed on a support for microscopic viewing.

The Vickers hardness was obtained using a Type M Shimadzu microhardness tester, following the ISO 6507 norm, employing a Vickers pyramidal indenter loaded onto the material surface with 50 g during 5 s and 100 g during 10 s, for PLA and PHBV and PLA containing blends, respectively. Each measurement is repeated 6 times to get accurate results.

DSC curves were obtained in a TA Instruments Q20 calorimeter and phase-transition parameters were determined using TA Universal Analysis software. Around 5 mg of sample weight were subjected in N_2 atmosphere, with a N_2 flow rate of 50 mL/min, to two consecutive cycles of heating-cooling: heating step (30 to 200 °C at 5 °C/min), isotherm at 200 °C for 3 min, cooling step (200–0 °C at 5 °C/min) and 3 min at 0 °C. As for thermal stability, it was studied by thermogravimetric analysis (TGA) with a TA Instruments TGA2050 thermobalance. The temperature program (40–800 °C, 10K/min ramp rate) was applied to samples of 12±1 mg under inert atmosphere (30 mL/min of N_2).

Layer thicknesses were measured with a digital coating thickness meter CM-8820 AMTAST (United States), averaging at least 6 measurements.

The O_2 barrier properties were measured following the standard ASTM D-3985 at 30 ± 0.5 °C, using a homemade O_2 permeator setup which has been previously described (Beltrán et al., 2017). The device essentially consists of a permeation cell with two chambers, separated by the monolayer or multilayer evaluated. O_2 permeability of the different samples is determined by means of diffusion experiments through the initially purged membrane. The permeability coefficient, P, was estimated from the pressure changes measured on the low-pressure side of the membrane, using an e-BARATRON digital manometer (MKS, USA). The confidence interval with this setup (at a confidence level of 95 %), estimated from 3 measurements, is lower than 5 %.

Light transmissions were determined by means of a Cary 1E UV–Vis spectrophotometer, at a scanning speed of 400 nm/min. Thickness of the tested bilayers and trilayers was 200 ± 15 μm, and all the transmission spectra were normalised to a sample thickness of 200 μm. The overall light transmission in the visible region (400–800 nm) was calculated from the normalised spectra, according to the ISO 13,468 standard, by using air as 100 % transmission reference.

3. Results and discussion

Considering the low compatibility between CH and biopolyesters such as PLA and PHBV, which has been widely reported in the literature (Andrade-Del Olmo et al., 2019; Vesel, 2023; Yovcheva et al., 2018), the first stage in obtaining materials based on biopolyester and CH layers was the surface activation of the polymers to improve adhesion. The different multilayer materials were then obtained and characterised, and the changes in permeability and optical properties were analysed.

3.1. Surface activation

The changes produced in the material by the activation processes were studied by DSC, FTIR-ATR and contact angle measurements. While FTIR-ATR and contact angle, data reveal only the changes taking place on the surface, DSC results correspond to the material as a whole.

3.1.1. DSC

Fig. 3 shows the DSC curves (first and second heating scans) corresponding to the activation of the films with NaOH. The DSC curves of PLA show three characteristic peaks. First, a well-defined endothermic peak that appears around 60 °C, in the first heating scans, can be associated to the physical aging of the material (Beltrán et al., 2016), and therefore does not reveal changes in its chemistry. It also appears a step close to this peak as a sudden change in heat capacity of the material. This change, which is clearly observed in the second heating scans (See Fig. 3c), is related to glass transition (Tg) (Beltrán et al., 2016). The insert in Fig. 3c shows that Tg (60 °C) does not change on activation. The peak that appears near 90 °C corresponds to cold crystallisation, and finally, at a temperature above 170 °C, the melting endotherm appears. These peaks, which correspond to the formation and melting of the crystalline phases of the material, allows the determination of the crystallinity of the polymer.

Fig. 3a shows that surface activation treatments of PLA with NaOH, at least for the short times used in this work, do not cause substantial changes in the micro-structure of the whole material, since the values of melting and cold crystallisation temperatures do not change significantly. The crystallinity values estimated according to Eq. (1) indicated neglectable increase, concisely, changing from 38 to 42 % after 60 min of activation treatment, since this treatment is superficial and do not intakes notorious changes in the bulk material. The change in crystallisation can be explained as a consequence of the chain scission caused by NaOH-catalysed hydrolysis, since the shorter chains formed have greater mobility and capacity to form crystalline structures. The phenomenon of NaOH-catalised PLA hydrolysis has been observed by different authors (Andrade-Del Olmo et al., 2019; Scaffaro et al., 2019). However, in this case the small changes observed in the crystallinity degree indicate that the changes in the polymeric micro-structure are minor.

Fig. 3b shows that the results are very similar for the PLA-PHBV blend. Again, the characteristic temperatures and the areas under the curves are very similar before and after the activation process, indicating that this activation method does not cause substantial changes in the overall micro-structure of the polymer.

3.1.2. FTIR-ATR

The effects of the activation processes on the surface chemical composition of the films were studied by FTIR-ATR spectroscopy. Fig. 4 shows the $C = O$ stretching region (1800–1700 cm^{-1}) in PLA films subjected to treatment with NaOH for different time periods. All spectra were normalised using the 1451 cm^{-1} band as an internal standard reference (Kister et al., 1998).

Fig. 4 reveals a slight shift to lower wavenumbers of the $C = O$ band

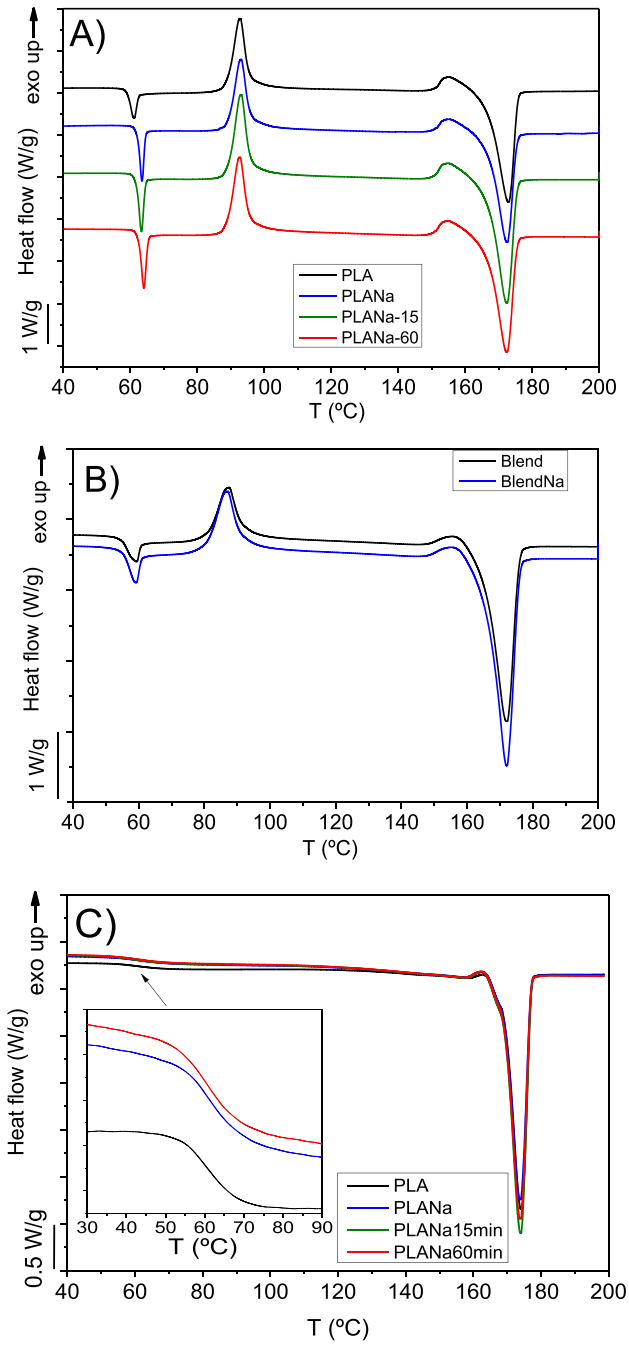

Fig. 3. DSC curves (first heating scan) of virgin and activated polymers. A: PLA, B: Blend. C: second heating scans of PLA activated samples.

as the exposure time increases. The formation of carboxyl (-COOH) groups during the NaOH-catalysed hydrolytic degradation of PLA may help to explain this shift, since the $C = O$ stretching vibration in -COOH groups appears at lower wavenumbers (Izumi & Temperini, 2010). Moreover, these -COOH groups can form hydrogen bonds with the ester groups, thus contributing to the shift. This result confirms the successful generation of carboxylic groups at the surface, as an effect of chemical activation with NaOH, as showed in Fig. 2, which increases hydrophilicity and promotes the compatibility between the CH coating and the PLA films, since the remaining amine groups of chitosan polymeric chains (showed in Fig. 1), can react with the surface -COOH groups of PLA (Nyanhongo et al., 2013). Similar results were obtained for the activation of the blend. In this case, the spectrum shows, in addition to the characteristic $C = O$ stretching band of PLA at 1750 cm^{-1}, an analogous band of the crystalline structures of PHBV at 1720 cm^{-1} (Bernabé Vírseda et al., 2024). After the activation with NaOH, it is also observed a shift to lower wavenumbers.

3.1.3. Contact angle and microhardness

Changes in the surface chemistry of the polymers during the activation process were also studied by measuring contact angle values, which are directly related to surface characteristics such as polarity and hydrophilicity and, hence, to properties such as adhesion and wettability (Gartner et al., 2015; Ščetar et al., 2017). PLA and PHBV surfaces show a hydrophobic nature, as corresponds to its chemical nature (Fig. 1), which limits the adhesion to polar coatings such as those based on chitosan.

Table 2 shows the contact angle and microhardness values measured

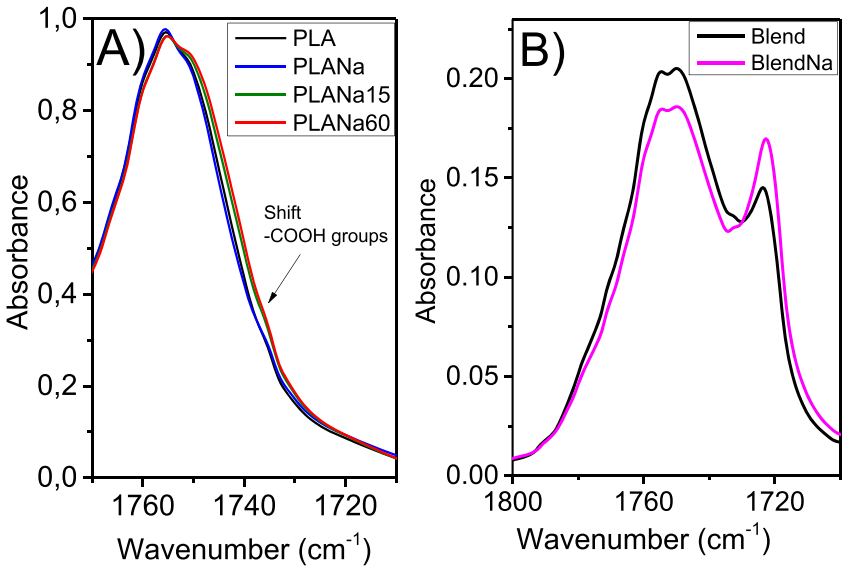

Fig. 4. FTIR-ATR spectra of PLA and PLA/PHBV Blend in the $C = O$ stretching region, before and after activation with NaOH.

Table 2
Contact angles and microhardness measured in virgin and activated PLA and Blend monolayers.

Sample	Contact angle (°)	Microhardness (MPa)
PLA	87.8 ± 2.4	210±29
PLANa	71.3 ± 7.7	218±20
PLANa-15	63.7 ± 4.2	285±24
PLANa-60	67.8 ± 5.2	304±30
PLANaCH	58.6 ± 2.9	–
Blend	83.0 ± 4.2	137±11
BlendNa	62.1 ± 1.9	212±32

before and after the treatment of the surfaces with aqueous NaOH. An example of a contact angle measured after the application of a layer of chitosan, also included in Table 2, shows that chitosan is more polar than PLA or PHBV, as can be expected from their respective chemical natures. The clear decrease observed in the contact angle values of the treated polymer surfaces indicates an increase in the polarity and hydrophilicity of the surface, which can be explained as a consequence of the NaOH-catalysed ester bond cleavage that leads to the formation of -COOH and -OH groups on the polymer surface. This result is consistent with the results obtained by FTIR spectroscopy, which show the formation of -COOH groups on the activated surfaces, as showed in Fig. 4.

The results collected in Table 1 also show that long times are not required for surface activation with this method, since the same surface modification is achieved in the first 5 min as in 60 min. Activation also takes place on the surface of the PLA+PHBV containing blend; in this case, an even greater decrease in the contact angle is achieved in the first 5 min. The introduction of polar groups and the decrease in contact angle confirm the effectiveness of this simple and affordable method for modifying the surface of biopolyesters such as PLA and PHBV, which can be expected to result in an improvement of the adhesion of thin chitosan layers.

Regarding the mechanical properties of the surface of the polymeric sheets after activating with NaOH, the results evidence the increase in hardness, especially after 15 min of activation, 35 %, compared to the PLA film not subjected to activation. Nevertheless, 5 min activation does not alter notoriously the surface hardness of PLA films. It is in good agreement with the slight changes in crystallinity estimated from DSC experiments (See Fig. 3), since crystallinity has a direct correlation to rigidity parameters, like hardness (Beltrán, Lorenzo et al., 2016; L. Wang et al., 2016). Changes in crystallinity are smaller than those observed in microhardness because the crystallinity measured by DSC corresponds to the entire material, while the microhardness corresponds only to the surface of the material.

3.1.4. Thermal stability

Thermal stability, a property that plays an important role in the processing and recycling of polymeric materials, has been studied by thermogravimetric analysis. The stability of different materials has been compared using two widely used parameters: T_{10}, the temperature at which 10 % of the mass is lost, which is often considered as an initial degradation temperature, and T_{max}, the temperature at which the rate of mass loss reaches the maximum. (Beltrán et al., 2018; Beltrán, Lorenzo et al., 2016)

Untreated PLA shows a single decomposition process, with T_{10} and T_{max} values of 342 and 373 °C, respectively. The PLA/PHBV blend shows a significantly lower T_{10} value, 294 °C, due to the lower thermal stability of PHBV. Regarding the effect of the treatments, activation with NaOH for 5 min produces no significant changes in PLA's T_{10} and T_{max}, and only minor changes, <5 °C, in the case of the blend activation, indicating that the polymer degradation occurring under these conditions is very minor, in good agreement with the DSC results. No significant effect of CH was also observed, although it should be noted that the amount of CH in the material is very small. Thus, the results indicate that neither the introduction of thin layers of CH nor the activation of PLA under mild conditions significantly impairs the stability of PLA or PHBV. (Beltrán, Lorenzo et al., 2016; Bernabé et al., 2024; Bernabé Vírseda et al., 2024)

3.1.5. Morphology

The changes in the morphology of the polymer surface due to activation treatments and the application of thin layers of chitosan, as well as the morphology of the PLA-chitosan interface, have been studied by scanning electron microscopy. Fig. 5a-b shows SEM images corresponding to the surface of untreated PLA and PLA subjected to NaOH activation for different times. The high-resolution images reveal the changes in the polymer surface nanostructures.

The main result of NaOH activation is surface etching, which causes a visible increase in roughness. This effect increases with treatment time, but is clearly noticeable even with mild treatment at 25 °C for 5 min. The application of a thin layer of CH causes a smoothing of the surface, which is observed in the SEM image of PLANaCH (Fig. 5.d). The smoothing due to the CH layer is also observed in the cross-sectional

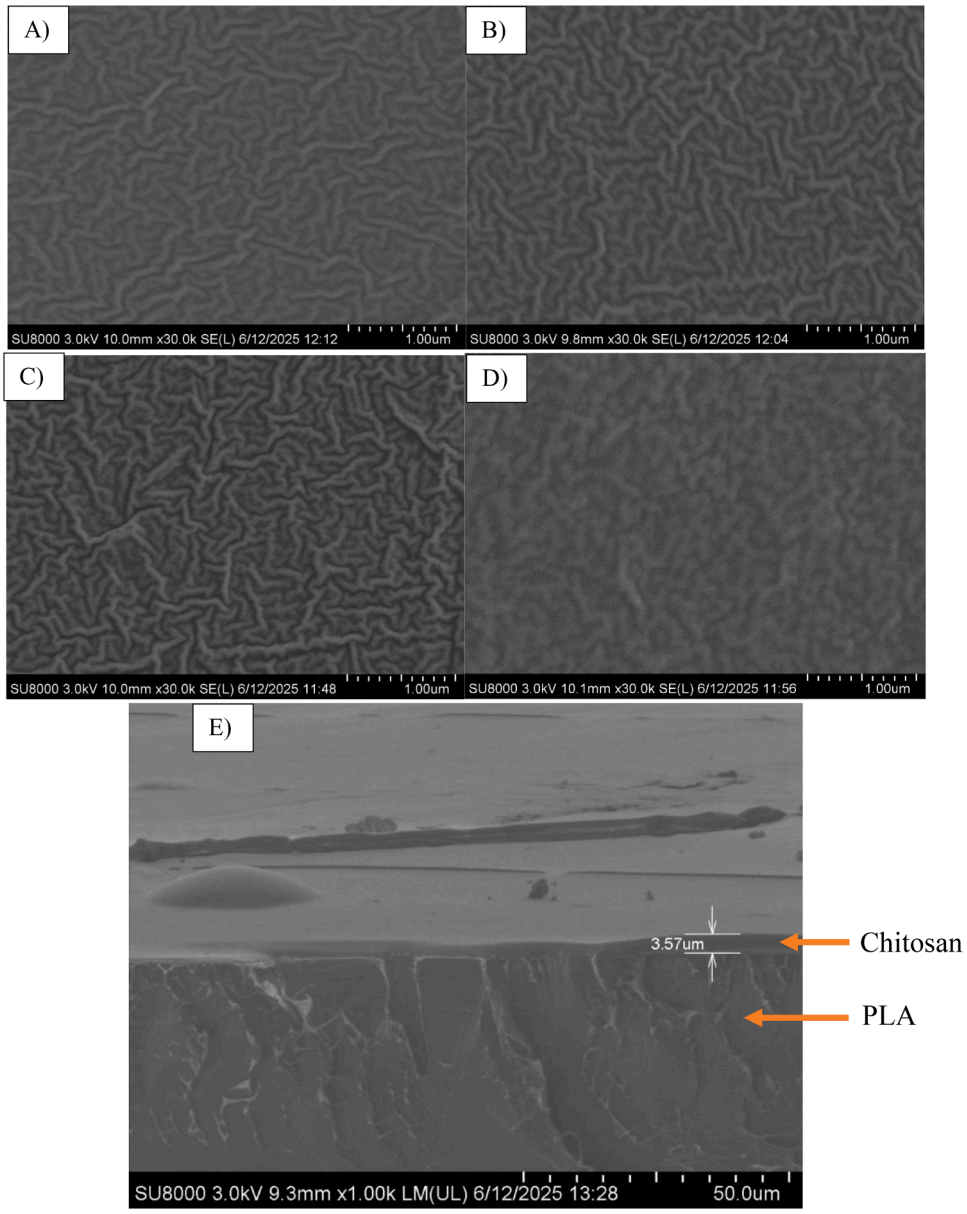

Fig. 5. SEM images of A) PLA, B) PLANa C) PLANa-15 and D) PLANaCH surfaces. E) Cross-section of PLANaCH sample.

image of PLANaCH, taken on a cryofractured surface (Fig. 5.e). (Gerard & Budtova, 2012; Liu et al., 2015; Mohd Sabee et al., 2016; Scaffaro et al., 2019) The CH coating is observed in the cross-section pictures, as phase-separated morphology, showing no space between chitosan layer and the PLA film, proving the proper adhesion between these components of the film, and consequently supporting FT-IR and contact angle results (See Table 2 and Fig. 4) referring the efficiency of the activation method followed in this research (Scaffaro et al., 2019)

3.2. CH coating onto biopolymeric films: chemistry, barrier and optical properties

The first step in obtaining the multilayers was the deposition on PLA sheets of a thin layer of CH from aqueous solutions of lactic acid (LA). Oligomeric lactic acid (OLA) was also added to the solution in some tests. In addition to the CH concentration, the volume of solution deposited was also varied, but high volumes were quickly discarded because they led to irregular CH coating along the sheets and did not improve the O_2 barrier. The thickness of the CH film was 8.0 ± 7.0 μm when a 1 wt. % solution of CH was used, and 9.8 ± 5.1 μm when the concentration was 2 wt. %.

Fig. 6 shows the FTIR-ATR spectra of a PLA film subjected to surface activation before (PLANa) and after (PLANaCH) being coated with CH. The spectrum of the coated sheet shows the characteristic CH bands, among which the bands at 3300, 1730 and 1575 cm^{-1} stand out. The broad band centred at 3300 cm^{-1} was assigned to the stretching modes of the N—H and O—H bonds of CH. The band at 1730 cm^{-1} reveals the presence of excess LA (Dou et al., 2020; Ube et al., 2017). The band centred at 1575 cm^{-1} presents a complex structure indicating the combination of different absorption bands that can be assigned, according to the literature, to different species present in the CH layer.

The shoulder observed at 1630 cm^{-1} could be due to the presence of the amide I band of the amide groups that remain in CH after the partial N-deacetylation of chitin (Pawlak & Mucha, 2003; Urreaga & de la Orden, 2006). The amide I band could also correspond to amides formed by the reaction of LA with CH, since Xin et al. have previously observed this formation reaction (Xin et al., 1999). However, in our case the entire dissolution and drying process was carried out under milder conditions,

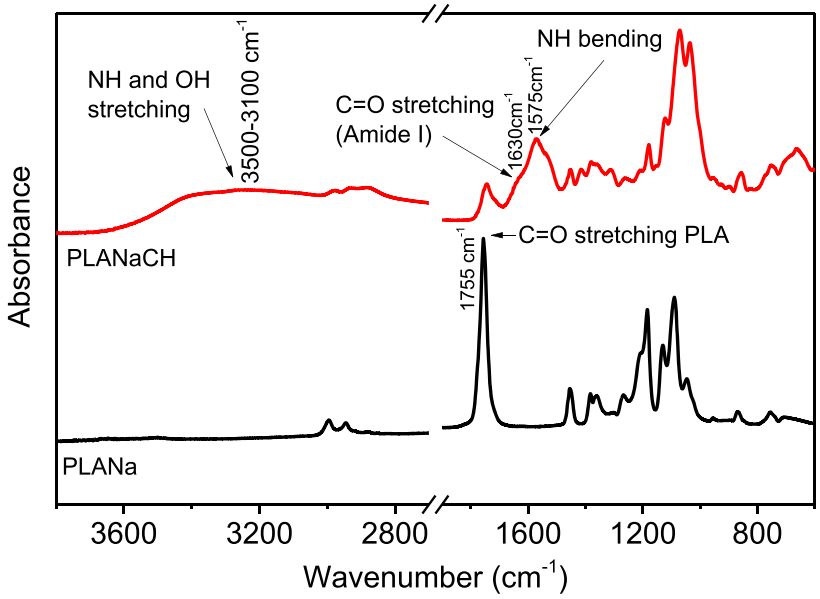

Fig. 6. FTIR-ATR spectra of PLANa and PLANaCH.

at 40 °C, than those used by the cited authors, who worked at 80 °C. Finally, the appearance at 1630 cm^{-1} of an absorption corresponding to the $-NH_3^+$ groups formed in the dissolution process of CH in an acidic medium has also been previously reported (Bacsik & Hedin, 2016). The band at 1575 cm^{-1} can be assigned to a bending mode of the $-NH_2$ groups still present in CH after the dissolution process (Urreaga & de la Orden, 2006), although characteristic absorptions of amide and $-NH_3^+$ groups may also contribute (Xin et al., 1999).

The multilayer materials obtained by compression moulding from PLANa, PLANaCH and BlendNa were characterised by FTIR micro-spectroscopy and microscopy. Fig. 7 shows a micrograph and the representative spectra of the PLANa-CHx1v1-PLANa trilayer. In this case, a well-defined thin layer is observed between the two outer layers. While the spectrum of the outer layers confirms that it is PLA, the spectrum of the intermediate barrier layer shows the characteristic bands of the CH layer as shown above in the FT-IR analysis (Fig. 5), especially the complex absorption band between 1500 and 1670 cm^{-1} and the band at 1735 cm^{-1}. These results therefore confirm that the procedures used allow obtaining multilayer materials with thin CH barrier layers in the structure.

3.3. O_2 permeability

To reduce O_2 permeation is essential for developing the use of materials such as PLA and PHBV in food packaging. In order to achieve this reduction, it is important to understand the gas permeation through polymeric films. It is composed of 4 steps: sorption of gas molecules onto the film surface, dissolution of the gas into the polymer, diffusion of the gas through the solid polymeric phase and gas desorption from the opposite surface of the film (Michiels et al., 2017; Râpă et al., 2016;

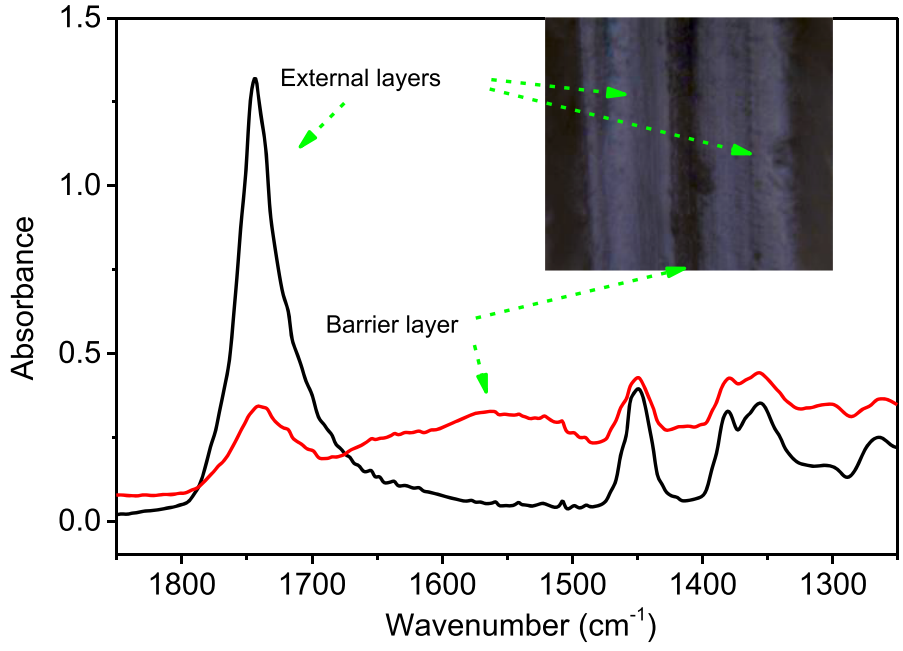

Fig. 7. Photomicrograph and FTIR spectra of the trilayer PLANa-CHx1v1-PLANa.

Zembouai et al., 2013). In partially crystalline polymers, such as PLA and PHBV, permeability depends primarily on the diffusion coefficient and the gas solubility and the permeability coefficient is considered to be the product of the diffusion coefficient and the solubility (Beltrán et al., 2018). Both parameters depend on the polymer structure, with key factors such as crystallinity and free volume. The permeability of materials like PLA can be reduced by adding layers of less permeable materials, such as chitosan, or by introducing additives or copolymers that increase crystallinity and reduce the free volume of the polymer.

In this work, we have studied the effect of CH thin internal layers of different thicknesses and compositions on the O_2 permeability of bilayers obtained from NaOH-activated films of PLA and PLA-PHBV blend (Fig. 8).

As can be observed in Fig. 8, the O_2 permeability decreases markedly with the addition of a thin film of CH between the two layers. The best result is obtained in the sample PLANa-CHx1v1-PLANa, which contains the thinnest layer of CH. In this case, the decrease in O_2 permeability, with respect to that of the PLANa-PLANa bilayer, reaches 75 %. It is also observed that increases in the thickness of the CH layer, caused either by the use of more concentrated solutions or by the use of larger solution volumes in the application of the CH layer, lead to worse results, with higher permeabilities, as can be seen in the samples PLANa-CHx1v2-PLANa and PLANa-CHx2v1-PLANa. However, in the worst case, the inner CH layer still reduces by 15 % the permeability of the PLANa-PLANa bilayer. These results, which can perhaps be explained as a result of thinner layers also being more regular and uniform, confirm that controlling the thickness of the CH coating is a key to obtaining better barrier properties of the film.

The introduction of OLA into the CH layer formulation also has a clearly negative effect on permeability, since the sample with OLA (PLANa-COx1v1-PLANa) shows a 100 % increase in permeability compared to the same sample without OLA (PLANa-CHx1v1-PLANa). This result appears to indicate that the use of OLA leads to the appearance of pores and ruptures in the CH layer, which promotes the formation of preferential channels and facilitates the flow of O_2 (Bastarrachea et al., 2011)

Concerning the PLA and Blend multilayers, Fig. 8 shows that the introduction of 25 wt. % PHBV in one of the layers allows a 44 % decrease in the O_2 permeability. This result coincides with those reported by different authors, who have always observed that the addition of PHBV reduces the permeability of PLA (Marano et al., 2022; Zembouai et al., 2013). For example, Zembouai et al. reported a 35 % decrease, similar to our 44 % decrease, in the O_2 permeability of PLA when introducing 25 wt. % PHBV in the blend (Zembouai et al., 2013). To explain this result, it must be considered that, on the one hand, PHBV has a much lower oxygen permeability than PLA due to its superior ratio of crystalline phase over amorphous areas. On the other hand, the effect of PHBV on the PLA micro-structure must also be considered. Jost and Kopitzky have reported that PHBV polymeric chains interpenetrate the PLA polymeric array, which leads to a decrease in free volume, causing a drop in the mobility inside the polymer, which contributes to the decrease in permeability (Jost & Kopitzky, 2015).

The use of a thin inner CH layer also reduces the oxygen permeability of the bilayers PLANa-BlendNa. In this case the decrease in permeability is around 50 %. It should be noted that the permeability of this PLANa-CHx1v1-BlendNa multilayer is very similar to that of the equivalent PLA-CH-PLA setup, as can be seen in Fig. 8, indicating that the inner CH layer plays a fundamental role in controlling the permeability of these multilayer polymeric films. Finally, it is also worth noting that the effect of the inner CH layer on the performance and applications of PLA can be important, since the permeability of the multilayers obtained is similar to that of PET (Michiels et al., 2017), a polymer widely used in food packaging.

3.4. UV–Visible transmission

Light transmission, both ultraviolet (UV) and visible (Vis), is very important in materials used in food packaging, because it is related to the stability and duration of the packaged foods and to the possibility of their observation by the customer. Light transmission is controlled by physical methods such as absorption, scattering, and reflection. In polymeric materials, these phenomena depend on the presence of substances with specific absorption properties and also on the presence of particles with a different refractive index than the matrix and the appropriate size, equal to or greater than the wavelength of the radiation, to cause reflection or scattering phenomena (Alizadeh Sani et al., 2024; Ezati et al., 2023; Worku et al., 2024). Fig. 9 shows the transmittance between 200 and 800 nm of different polymer multilayers developed in this work, together with digital photographs of the same materials that visually show their transparency. The spectra confirm that the structures containing only PLA have high transmission in the visible range and good transparency, which is very suitable for food packaging. However, UV transmission is also high, which leads to weak protection of food against UV-induced degradation and limits the application of PLA in food packaging (Mao et al., 2022, 2025).

The addition of a thin inner layer of CH reduces the transmission of the PLANa-PLANa bilayer from 75 to 64 % in the full UV–Vis range, but the effect is different in the two regions. While the transmission in the

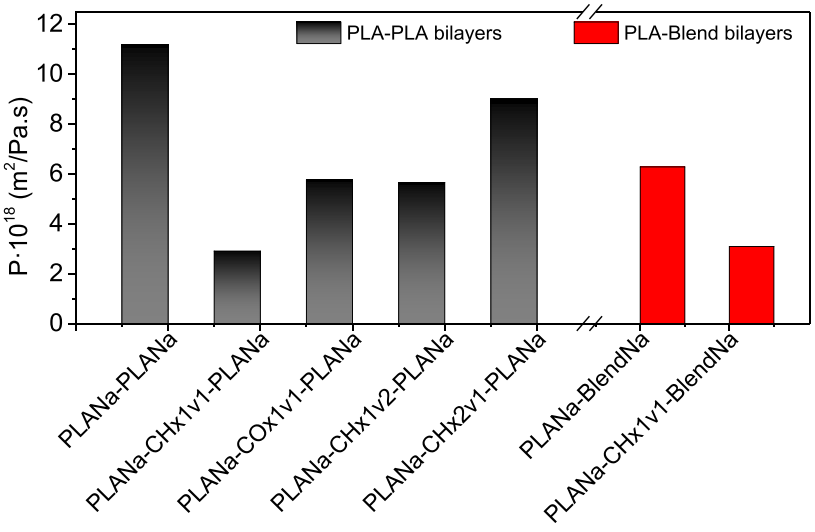

Fig. 8. Effect of thin internal layers of CH on the O_2 permeability of PLA and Blend multilayers.

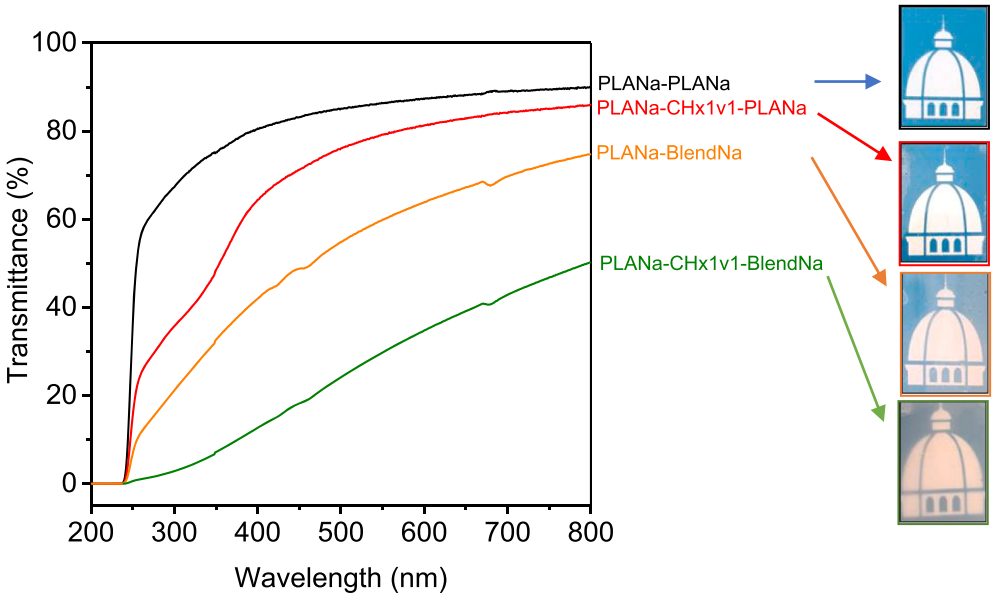

Fig. 9. UV–Visible transmission of representative bilayer and trilayer films.

visible range is only slightly reduced, and the material still displays good transparency, the transmission in the UV region of the spectrum is reduced to a greater extent, which contributes to increasing the UV barrier of the material and therefore its suitability for food packaging.

Fig. 9 also shows that the light transmission is much lower in the PLA-Blend bilayer, both in the visible and UV ranges. Even though the presence of PHBV only reaches 25 wt. % in one of the two layers, it causes a decrease in transmission to 48 %, compared to 75 % for the PLANa-PLANa bilayer. The spectrum of the PLANa-BlendNa bilayer shows the absence of specific absorption bands in the material, so the decrease in transmittance must be explained by analysing the microstructure of the blend and the miscibility between both polymers.

The miscibility of PLA and PHBV depends on the molecular weight of each polymer and the percentage of the minor component in the blend (Jost & Kopitzky, 2015; Marano et al., 2022). However, several authors have shown that the commercial grades of both polymers, with high molecular weight, are not miscible regardless of the composition of the blend (Gerard & Budtova, 2012; Liu et al., 2015; Zembouai et al., 2013). Gerard & Budtova showed that PHBV forms droplets in the PLA matrix of average diameter 1.2 μm when the PHBV content is 30 % by weight (Gerard & Budtova, 2012). Considering that PLA and PHBV have different refractive indices, multilayers of this size can effectively disperse UV and visible radiation, thus contributing to the decrease in transmittance. Furthermore, it is also known that PHBV particles can induce the crystallisation of PLA, thus generating crystalline phases that can also contribute to dispersing light and reducing transmittance (Liu et al., 2015). The high dispersion of visible light also explains the haze observed in digital photographs corresponding to multilayer containing PHBV.

The addition of a thin inner layer of CH, as observed in SEM (See Fig. 5), causes a further decrease in the transmittance of the structures with PHBV, which is reduced to 24 % between 200 and 800 nanometers. An increase in turbidity is also observed. On the positive side, the presence of CH leads to a very high blocking of UV radiation, which can contribute to increasing the shelf life of packaged foods, since UV radiation is involved in photochemical reactions in food products that cause changes in colour, flavour and textures, as well as nutritional quality degradation (Alizadeh Sani et al., 2024; Ezati et al., 2023; Hellwig, 2019; Tripathi et al., 2024; Worku et al., 2024).

4. Conclusions

In this work, multilayer sheets have been successfully developed from PLA and PLA-PHBV blend films, with thin internal layers of chitosan (CH), in order to reduce the O_2 permeability without impairing the optical properties of the material. The hydrophobic surfaces of the polymers were activated with aqueous NaOH to modify the chemical surface of the material and improve the adhesion with the hydrophilic CH. A treatment time of only 5 min at 25 °C was sufficient to generate polar groups such as -COOH on the polymer surface and reduce the contact angle with water a 18 %, without causing an apparent degradation of the polymer. The presence of 25 wt. % PHBV in one of the films leads to a decrease in O_2 permeability of 44 %, together with a 36 % reduction in UV–Vis transmittance, but the reduction takes place in both the ultraviolet and visible ranges and leads to a detrimental decrease in transparency. These results are explained as a consequence of the poor miscibility between PLA and PHBV. The addition of a thin layer of CH, leads to a 75 % decrease in O_2 permeability and an interesting decrease of 15 % in UV–Vis transmittance of PLA-PLA bilayers. Furthermore, in this case the reduction occurs mainly in the ultraviolet range, so it does not significantly affect the transparency of the material in the visible range.

CRediT authorship contribution statement

I. Bernabé Vírseda: Writing – original draft, Methodology, Investigation, Formal analysis, Data curation. **M.U. de la Orden:** Writing – review & editing, Validation, Supervision, Conceptualization. **J. Martínez Urreaga:** Writing – review & editing, Validation, Supervision, Project administration, Methodology, Funding acquisition, Conceptualization.

Declaration of competing interest

The authors declare that they have no known competing financial interests or personal relationships that could have appeared to influence the work reported in this paper.

Acknowledgements

Authors received funding from European Union's Horizon 2020

research and innovation program under grant agreement No. 860407 BIO-PLASTICS EUROPE and Universidad Politécnica de Madrid (Project UPM RP2205430163). Also, authors gratefully acknowledge Prof. Aurora Lasagabaster Latorre (Facultad de Óptica y Optometría, Universidad Complutense de Madrid, Spain), for the help and assistance with the FT-IR microspectroscopy; Dr. Simon Gölden for the help and collaboration for the GPC measurements (Fraunhofer LBF Institute, Darmstadt, Germany) and David Gómez (ICTP-CSIC, Madrid, Spain), for the assistance and collaboration in the FE-SEM measurements.

Data availability

Data will be made available on request.

References

Alizadeh Sani, M., Khezerlou, A., Tavassoli, M., Abedini, A. H., & McClements, D. J (2024). Development of sustainable UV-screening food packaging materials: A review of recent advances. *Trends in Food Science & Technology, 145*, Article 104366. https://doi.org/10.1016/j.tifs.2024.104366

Andrade-Del Olmo, J., Pérez-Álvarez, L., Hernáez, E., Ruiz-Rubio, L., & Vilas-Vilela, J. L. (2019). Antibacterial multilayer of chitosan and (2-carboxyethyl)- β-cyclodextrin onto polylactic acid (PLLA). *Food Hydrocolloids, 88*, 228–236. https://doi.org/10.1016/j.foodhyd.2018.10.014

Anukiruthika, T., Sethupathy, P., Wilson, A., Kashampur, K., Moses, J. A., & Anandharamakrishnan, C. (2020). Multilayer packaging: Advances in preparation techniques and emerging food applications. *Comprehensive Reviews in Food Science and Food Safety, 19*(3), 1156–1186. https://doi.org/10.1111/1541-4337.12556

Bacsik, Z., & Hedin, N. (2016). Effects of carbon dioxide captured from ambient air on the infrared spectra of supported amines. *Vibrational Spectroscopy, 87*, 215–221. https://doi.org/10.1016/j.vibspec.2016.10.006

Bastarrachea, L., Dhawan, S., & Sablani, S. S. (2011). Engineering properties of polymeric-based antimicrobial films for food packaging: A review. *Food Engineering Reviews, 3*(2), 79–93. https://doi.org/10.1007/s12393-011-9034-8

Beltrán, F. R., Climent-Pascual, E., de la Orden, M. U., & Martínez Urreaga, J. (2020). Effect of solid-state polymerization on the structure and properties of mechanically recycled poly(lactic acid). *Polymer Degradation and Stability, 171*. https://doi.org/10.1016/j.polymdegradstab.2019.109045

Beltrán, F. R., de la Orden, M. U., Lorenzo, V., Pérez, E., Cerrada, M. L., & Martínez Urreaga, J. (2016a). Water-induced structural changes in poly(lactic acid) and PLLA-clay nanocomposites. *Polymer, 107*, 211–222. https://doi.org/10.1016/j.polymer.2016.11.031

Beltrán, F. R., Lorenzo, V., Acosta, J., de la Orden, M. U., & Martínez Urreaga, J. (2018). Effect of simulated mechanical recycling processes on the structure and properties of poly(lactic acid). *Journal of Environmental Management, 216*, 25–31. https://doi.org/10.1016/j.jenvman.2017.05.020

Beltrán, F. R., Lorenzo, V., de la Orden, M. U., & Martínez-Urreaga, J. (2016b). Effect of different mechanical recycling processes on the hydrolytic degradation of poly(l-lactic acid). *Polymer Degradation and Stability, 133*, 339–348. https://doi.org/10.1016/j.polymdegradstab.2016.09.018

Beltrán, F. R., Ortega, E., Solvoll, A. M., Lorenzo, V., de la Orden, M. U., & Martínez Urreaga, J. (2017). Effects of aging and different mechanical recycling processes on the structure and properties of poly(lactic acid)-clay nanocomposites. *Journal of Polymers and the Environment*. https://doi.org/10.1007/s10924-017-1117-z

Bernabé, I., Amarilla, E., de la Orden, M. U., Martínez Urreaga, J., & Beltrán, F. R. (2024). Effect of oligomeric lactic acid plasticizer on the mechanical recycling of poly(3-hydroxybutyrate-co-3-hydroxyvalerate). *Environmental Science and Pollution Research*. https://doi.org/10.1007/s11356-023-31758-0. *0123456789*.

Bernabé Vírseda, I., Beltrán, F. R., de la Orden, M. U., & Martínez Urreaga, J. (2024). Effects of solid-state polymerization on the structure and properties of degraded poly (3-hydroxybutyrate-co-3-hydroxyvalerate). *Polymer Degradation and Stability, 220*, Article 110630. https://doi.org/10.1016/j.polymdegradstab.2023.110630

Claro, P. I. C., Neto, A. R. S., Bibbo, A. C. C., Mattoso, L. H. C., Bastos, M. S. R., & Marconcini, J. M. (2016). Biodegradable blends with potential use in packaging: A comparison of PLA/chitosan and PLA/cellulose acetate films. *Journal of Polymers and the Environment, 24*(4), 363–371. https://doi.org/10.1007/s10924-016-0785-4

Dou, X., Li, Q., Wu, Q., Duan, L., Zhou, S., & Zhang, Y. (2020). Effects of lactic acid and mixed acid aqueous solutions on the preparation, structure and properties of thermoplastic chitosan. *European Polymer Journal, 134*. https://doi.org/10.1016/j.eurpolymj.2020.109850

Ezati, P., Khan, A., Priyadarshi, R., Bhattacharya, T., Tammina, S. K., & Rhim, J.-W. (2023). Biopolymer-based UV protection functional films for food packaging. *Food Hydrocolloids, 142*, Article 108771. https://doi.org/10.1016/j.foodhyd.2023.108771

Gartner, H., Li, Y., & Almenar, E. (2015). Improved wettability and adhesion of polylactic acid/chitosan coating for bio-based multilayer film development. *Applied Surface Science, 332*, 488–493. https://doi.org/10.1016/j.apsusc.2015.01.157

Gerard, T., & Budtova, T. (2012). Morphology and molten-state rheology of polylactide and polyhydroxyalkanoate blends. *European Polymer Journal, 48*(6), 1110–1117. https://doi.org/10.1016/j.eurpolymj.2012.03.015

Ghassemi, A., Moghaddamzadeh, S., Duchesne, C., & Rodrigue, D. (2017). Effect of annealing on gas permeability and mechanical properties of polylactic acid/talc composite films. *Journal of Plastic Film & Sheeting, 33*(4), 361–383. https://doi.org/10.1177/8756087917694618

Haghighi, H., Licciardello, F., Fava, P., Siesler, H. W., & Pulvirenti, A. (2020). Recent advances on chitosan-based films for sustainable food packaging applications. *Food Packaging and Shelf Life, 26*, Article 100551. https://doi.org/10.1016/j.fpsl.2020.100551

Hamad, K., Kaseem, M., Yang, H. W., Deri, F., & Ko, Y. G. (2015). Properties and medical applications of polylactic acid: A review. *Express Polymer Letters, 9*(5), 435–455. https://doi.org/10.3144/expresspolymlett.2015.42

Hellwig, M. (2019). The chemistry of protein oxidation in food. *Angewandte Chemie International Edition, 58*(47), 16742–16763. https://doi.org/10.1002/anie.201814144

Hosseini, S. F., Kaveh, F., & Schmid, M. (2022). Facile fabrication of transparent high-barrier poly(lactic acid)-based bilayer films with antioxidant/antimicrobial performances. *Food Chemistry*, 384. https://doi.org/10.1016/j.foodchem.2022.132540

Izumi, C. M. S., & Temperini, M. L. A. (2010). FT-raman investigation of biodegradable polymers: Poly(3-hydroxybutyrate) and poly(3-hydroxybutyrate-co-3-hydroxyvalerate). *Vibrational Spectroscopy, 54*(2), 127–132. https://doi.org/10.1016/j.vibspec.2010.07.011

Jost, V., & Kopitzky, R. (2015). Blending of polyhydroxybutyrate-co-valerate with polylactic acid for packaging applications - reflections on miscibility and effects on the mechanical and barrier properties. *Chemical and Biochemical Engineering Quarterly, 29*(2), 221–246. https://doi.org/10.15255/CABEQ.2014.2257

Kan, M., & Miller, S. A. (2022). Environmental impacts of plastic packaging of food products. *Resources, conservation and recycling* (p. 180). https://doi.org/10.1016/j.resconrec.2022.106156

Kister, G., Cassanas, G., & Vert, M. (1998). Effects of morphology, conformation and configuration on the IR and raman spectra of various poly(lactic acid)s. *Polymer, 39*(2), 267–273. https://doi.org/10.1016/S0032-3861(97)00229-2

Kumar, S., Dubey, N., Kumar, V., Choi, I., Jeon, J., & Kim, M. (2024). Combating micro/nano plastic pollution with bioplastic: Sustainable food packaging, challenges, and future perspectives. *Environmental Pollution, 363*, Article 125077. https://doi.org/10.1016/j.envpol.2024.125077

Laufer, G., Priolo, M. A., Kirkland, C., & Grunlan, J. C. (2013). High oxygen barrier, clay and chitosan-based multilayer thin films: An environmentally friendly foil replacement. *Green Materials, 1*(1), 4–10. https://doi.org/10.1680/gmat.12.00002

Liu, Q., Wu, C., Zhang, H., & Deng, B. (2015). Blends of polylactide and poly(3-hydroxybutyrate-co-3-hydroxyvalerate) with low content of hydroxyvalerate unit: Morphology, structure, and property. *Journal of Applied Polymer Science*, (42), 132. https://doi.org/10.1002/app.42689

Li, Y., Ren, J., Wang, B., Lu, W., Wang, H., & Hou, W. (2020). Development of biobased multilayer films with improved compatibility between polylactic acid-chitosan as a function of transition coating of SiOx. *International Journal of Biological Macromolecules, 165*, 1258–1263. https://doi.org/10.1016/j.ijbiomac.2020.10.001

Maga, D., Hiebel, M., & Thonemann, N. (2019). Life cycle assessment of recycling options for polylactic acid. *Resources, Conservation and Recycling, 149*, 86–96. https://doi.org/10.1016/j.resconrec.2019.05.018. April.

Mao, L., Bai, Z., Yao, J., & Liu, Y. (2022). Development of novel poly(lactic acid) active multilayer composite films by incorporating catechol-functionalized layered clay into chitosan/poly(vinyl alcohol) coatings. *Progress in Organic Coatings, 170*. https://doi.org/10.1016/j.porgcoat.2022.107000

Mao, L., Wang, C., Dong, Z. Y., Yao, J., Dong, F., & Dai, X. (2025). Fabrication of polylactic acid bilayer composite films using polyvinyl alcohol based coatings containing functionalized carbon dots and layered clay for active food packaging. *Industrial Crops and Products*, 225. https://doi.org/10.1016/j.indcrop.2025.120460

Marano, S., Laudadio, E., Minnelli, C., & Stipa, P. (2022). Tailoring the barrier properties of PLA: A State-of-the-art review for food packaging applications. *Polymers, 14*(8), 1626. https://doi.org/10.3390/polym14081626

Michiels, Y., Puyvelde, P., & Sels, B. (2017). Barriers and chemistry in a bottle: Mechanisms in today's oxygen Barriers for tomorrow's materials. *Applied Sciences, 7*(7), 665. https://doi.org/10.3390/app7070665

Mohd Sabee, M. M. S., Kamalaldin, N. A., Yahaya, B. H., & Abdul Hamid, Z. A. (2016). Characterization and in vitro study of surface modified PLA microspheres treated with NaOH. *Journal of Polymer Materials, 33*(1), 191–200.

Najahi, H., Banni, M., Nakad, M., Abboud, R., Assaf, J. C., Operato, L., Belhassen, M., Gomes, L., & Hamd, W. (2025). Plastic pollution in food packaging systems: Impact on human health, socioeconomic considerations and regulatory framework. *Journal of Hazardous Materials Advances, 18*, Article 100667. https://doi.org/10.1016/j.hazadv.2025.100667

Ncube, L. K., Ude, A. U., Ogunmuyiwa, E. N., Zulkifli, R., & Beas, I. N. (2020). Environmental impact of food packaging materials: A review of contemporary development from conventional plastics to polylactic acid based materials. *Materials, 13*(21), 1–24. https://doi.org/10.3390/ma13214994

Nyanhongo, G. S., Rodríguez, R. D., Prasetyo, E. N., Caparrós, C., Ribeiro, C., Sencadas, V., Lanceros-Mendez, S., Acero, E. H., & Guebitz, G. M. (2013). Bioactive albumin functionalized polylactic acid membranes for improved biocompatibility. *Reactive and Functional Polymers, 73*(10), 1399–1404. https://doi.org/10.1016/j.reactfunctpolym.2012.12.007

Park, S. H., Lee, H. S., Choi, J. H., Jeong, C. M., Sung, M. H., & Park, H. J. (2012). Improvements in barrier properties of poly(lactic acid) films coated with chitosan or chitosan/clay nanocomposite. *Journal of Applied Polymer Science, 125*(SUPPL. 1). https://doi.org/10.1002/app.36405

Pawariya, V., De, S., & Dutta, J. (2023). Synthesis and characterization of a new developed modified-chitosan Schiff base with improved antibacterial properties for the removal of Bismarck Brown R and Eosin Y dyes from wastewater. *Carbohydrate Polymer Technologies and Applications, 6*, Article 100352. https://doi.org/10.1016/j.carpta.2023.100352

Pawariya, V., De, S., & Dutta, J. (2024). Chitosan-based Schiff bases: Promising materials for biomedical and industrial applications. *Carbohydrate Polymers, 323*, Article 121395. https://doi.org/10.1016/j.carbpol.2023.121395

Pawlak, A., & Mucha, M. (2003). Thermogravimetric and FTIR studies of chitosan blends. *Thermochimica Acta, 396*(1–2), 153–166. https://doi.org/10.1016/S0040-6031(02)00523-3

Europe, Plastics (2024). Plastics - the fast facts 2024. *Plastics europe*.

Priyadarshi, R., & Rhim, J.-W. (2020). Chitosan-based biodegradable functional films for food packaging applications. *Innovative Food Science & Emerging Technologies, 62*, Article 102346. https://doi.org/10.1016/j.ifset.2020.102346

Rabeie, B., Mahmoodi, N. M., Hayati, B., Dargahi, A., & Rezakhani Moghaddam, H. (2024). Chitosan adorned with ZIF-67 on ZIF-8 biocomposite: A potential LED visible light-assisted photocatalyst for wastewater decontamination. *International Journal of Biological Macromolecules, 282*, Article 137405. https://doi.org/10.1016/j.ijbiomac.2024.137405

RameshKumar, S., Shaiju, P., O'Connor, K. E., & P, R. B (2020). Bio-based and biodegradable polymers - State-of-the-art, challenges and emerging trends. *Current Opinion in Green and Sustainable Chemistry, 21*, 75–81. https://doi.org/10.1016/j.cogsc.2019.12.005

Răpă, M., Miteluţ, A. C., Tănase, E. E., Grosu, E., Popescu, P., Popa, M. E., Rosnes, J. T., Sivertsvik, M., Darie-Niţă, R. N., & Vasile, C. (2016). Influence of chitosan on mechanical, thermal, barrier and antimicrobial properties of PLA-biocomposites for food packaging. *Composites Part B: Engineering, 102*, 112–121. https://doi.org/10.1016/j.compositesb.2016.07.016

ortunato Scaffaro, R., Maio, A., Sutera, F., Gulino, E., & Morreale, M. (2019). Degradation and recycling of films based on biodegradable polymers: A short review. *Polymers*, (4), 11. https://doi.org/10.3390/polym11040651.

Ščetar, M., Kurek, M., Režek Jambrak, A., Debeaufort, F., & Galić, K. (2017). Influence of high power ultrasound on physical-chemical properties of polypropylene films aimed for food packaging: Barrier and contact angle features. *Polymer International, 66*(11), 1572–1578. https://doi.org/10.1002/pi.5415

Schneider, M., Fritzsche, N., Puciul-Malinowska, A., Baliś, A., Mostafa, A., Bald, I., Zapotoczny, S., & Taubert, A. (2020). Surface etching of 3D printed poly(lactic acid) with NaOH: A systematic approach. *Polymers*, (8), 12. https://doi.org/10.3390/POLYM12081711

Stefaniak, K., & Masek, A. (2025). Poly(lactic acid) (PLA) – Short review of synthesis methods, properties, recent progress, and new challenges. *Express Polymer Letters, 19*(4), 386–408. https://doi.org/10.3144/expresspolymlett.2025.29

Stoleru, E., Vasile, C., Irimia, A., & Brebu, M. (2021). Towards a bioactive food packaging: Poly(Lactic Acid) surface functionalized by Chitosan coating embedding clove and argan oils. *Molecules, 26*(15), 4500. https://doi.org/10.3390/molecules26154500

Sundqvist-Andberg, H., & Åkerman, M. (2021). Sustainability governance and contested plastic food packaging – An integrative review. *Journal of Cleaner Production, 306*, Article 127111. https://doi.org/10.1016/j.jclepro.2021.127111

Teixeira, L. V., Bomtempo, J. V., Oroski, F., de, A., & Coutinho, P. L. (2023). The diffusion of bioplastics: What can we learn from Poly(Lactic Acid)? *Sustainability, 15*(6), 4699. https://doi.org/10.3390/su15064699

Tripathi, S., Kumar, L., Deshmukh, R. K., & Gaikwad, K. K. (2024). Ultraviolet blocking films for food packaging applications. *Food and Bioprocess Technology, 17*(6), 1563–1582. https://doi.org/10.1007/s11947-023-03221-y

Ube, T., Yoneyama, Y., & Ishiguro, T. (2017). In situ measurement of the pH-dependent transmission infrared spectra of aqueous lactic acid solutions. *Analytical Sciences, 33*, 1395–1400. https://doi.org/10.2116/analsci.33.1395

Urreaga, J. M., & de la Orden, M. U. (2006). Chemical interactions and yellowing in chitosan-treated cellulose. *European Polymer Journal*, (10), 42. https://doi.org/10.1016/j.eurpolymj.2006.05.002

Vesel, A. (2023). Deposition of Chitosan on plasma-treated polymers—A review. *Polymers, 15*(5), 1109. https://doi.org/10.3390/polym15051109

Wang, H., Qian, J., & Ding, F. (2018). Emerging Chitosan-based films for food packaging applications. *Journal of Agricultural and Food Chemistry, 66*(2), 395–413. https://doi.org/10.1021/acs.jafc.7b04528

Wang, L., Qiu, J., & Sakai, E. (2016). Microstructures and mechanical properties of polylactic acid prepared by a cold rolling process. *Journal of Materials Processing Technology, 232*, 184–194. https://doi.org/10.1016/j.jmatprotec.2016.02.006

Worku, L. A., Tadesse, M. G., Bachheti, A., Pandey, D. P., Chandel, A. K., Ewuntu, A. W., & Bachheti, R. K. (2024). Experimental investigations on PVA/chitosan and PVA/chitin films for active food packaging using Oxytenanthera abyssinica lignin nanoparticles and its UV-shielding, antimicrobial, and antiradical effects. *International Journal of Biological Macromolecules, 254*, Article 127644. https://doi.org/10.1016/j.ijbiomac.2023.127644

Xin, Q., Wirsén, A., & Albertsson, A. C. (1999). Synthesis and characterization of pH-sensitive hydrogels based on chitosan and D,L-lactic acid. *Journal of Applied Polymer Science, 74*(13), 3193–3202. https://doi.org/10.1002/(SICI)1097-4628(19991220)74, 13<3193::AID−APP23>3.0.CO;2-V.

Yin, Y., Zhou, J., Fu, H., Liu, S., Zhu, Q., Liao, C., & Jiang, G. (2025). Occurrence and migration of synthetic phenolic antioxidants in food packaging materials: Effects of plastic types and storage temperature. *Science of The Total Environment, 963*, Article 178459. https://doi.org/10.1016/j.scitotenv.2025.178459

Yovcheva, T., Viraneva, A., Marinova, A., Sotirov, S., Exner, G., Bodurov, I., Marudova, M., Pilicheva, B., Uzunova, Y., & Vlaeva, I. (2018). Insulating chitosan/casein multilayers on corona charged polylactic acid substrates. *IEEE Transactions on Dielectrics and Electrical Insulation, 25*(3), 766–771. https://doi.org/10.1109/TDEI.2017.006948

Zembouai, I., Kaci, M., Bruzaud, S., Benhamida, A., Corre, Y. M., & Grohens, Y. (2013). A study of morphological, thermal, rheological and barrier properties of poly(3-hydroxybutyrate-Co-3-Hydroxyvalerate)/polylactide blends prepared by melt mixing. *Polymer Testing, 32*(5), 842–851. https://doi.org/10.1016/j.polymertesting.2013.04.004